available at www.sciencedirect.com
journal homepage: www.eu-openscience.europeanurology.com

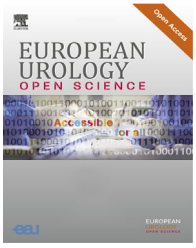

European Association of Urology

Bladder Cancer

Feasibility and Impact of Immunohistochemistry-based Molecular Subtyping for Muscle-invasive Bladder Cancer in Patients Treated with Radiation-based Therapy

Charles Hesswani[a], *Chelsea L. Jackson*[b], *Gautier Marcq*[a], *Céline Hardy*[b], *Ronald Kool*[a], *Jose Joao Mansure*[a], *Fadi Brimo*[c], *David M. Berman*[b], *Wassim Kassouf*[a,*]

[a] *Division of Urology, McGill University Health Centre, McGill University, Montreal, Canada;* [b] *Department of Pathology and Molecular Medicine, Queen's University, Kingston, Canada;* [c] *Department of Pathology, McGill University Health Centre, McGill University, Montreal, Canada*

Article info

Article history:
Accepted September 4, 2023

Associate Editor:
M. Carmen Mir

Keywords:
Antibody algorithm
Bladder cancer
Immunohistochemistry
Molecular subtype
Radiotherapy

Abstract

Background: Distinct molecular subtypes of muscle-invasive bladder cancer (MIBC) have been identified via gene expression profiling.
Objective: We investigated the feasibility of a simple immunohistochemistry (IHC)-based Lund subtyping method and the association of MIBC subtypes with oncological outcomes for patients after bladder-preserving radiation-based therapy.
Design, setting, and participants: Transurethral resected tumor tissues from 104 patients treated with radiation-based therapy were sampled on tissue microarray blocks.
Outcome measurements and statistical analysis: The expression of KRT5, GATA3, and p16 proteins was scored via digital image analysis. Hierarchical clustering was used to classify tumors as the basal subtype or one of two luminal subtypes: genomically unstable (GU) or urothelial-like (URO). Subtypes were evaluated for association with complete response (CR), recurrence-free survival (RFS), and overall survival (OS).
Results and limitations: The median OS was 43 mo (95% confidence interval 19–77) and median follow-up was 55 mo (interquartile range 39–75). Age and clinical stage had a significant impact on OS ($p < 0.05$). IHC-based subtype classification was feasible in most patients (89%). The subtype was basal in 23.6%, GU in 14.0%, URO in 31.2%, and unclassified in 31.2% of patients. No significant differences in CR, RFS, or OS were observed between the molecular subtypes. Limitations include the retrospective design and relatively small sample size.
Conclusions: IHC-based molecular MIBC subtyping using a three-antibody algorithm is feasible in most patients treated with radiation-based therapy. MIBC subtype was not associated with response or survival. Further prospective studies are warranted to confirm the lack of association between molecular subtype and survival in patients treated with trimodal therapy.

* Corresponding author. Division of Urology, McGill University Health Center, 1001 Decarie Boulevard, Montreal, Quebec H4A 3J1, Canada. Tel. +1 514 9348246.
E-mail address: wassim.kassouf.med@ssss.gouv.qc.ca (W. Kassouf).

https://doi.org/10.1016/j.euros.2023.09.003

Patient summary: For patients with invasive bladder cancer treated with radiation-based therapy, we classified tumors into different subtypes using just three molecular stains. This method is cheaper and more widely available than the usual approach. However, we did not find an association between different cancer subtypes and survival.

1. Introduction

Standard treatment for muscle-invasive bladder cancer (MIBC) is radical cystectomy (RC) followed by urinary diversion, with a 5-yr survival rate of 36–49% [1]. Given the morbidity associated with RC, bladder-sparing approaches such as trimodal therapy (TMT) are increasingly offered to selected candidates. TMT has shown comparable oncological outcomes to RC when patients are appropriately selected [2–4].

Subtyping of bladder cancer is an emerging approach, with specific subtypes linked to cancer progression, treatment responses, and metastasis rates [5,6]. In the last decade, several groups, including Lund University, The Cancer Genome Atlas, and MD Anderson Cancer Center, have subdivided bladder cancer into various subtypes according to mRNA expression profiling using specific markers [7–10]. The two major intrinsic subtypes, luminal and basal, show distinct clinical behaviors and responses to chemotherapy [5]. Basal urothelial cancers are associated with a more aggressive clinical course in comparison to luminal tumors, but may derive a greater survival benefit from platinum-based neoadjuvant systemic chemotherapy [11].

Although mRNA expression profiling is the gold standard for quantification of markers used to classify bladder cancer, it can be costly to perform and is not practical in many centers. Subtyping of bladder cancer using immunohistochemistry (IHC) is less costly and faster and is performed using antibody assays that are widely available in pathology laboratories [12,13]. The Lund classification scheme was first based on mRNA expression levels and was later refined using an IHC-based taxonomy validated against mRNA sequencing [14,15]. The subtypes identified included luminal genomically unstable (GU), luminal urothelial-like (URO), basal/squamous (basal), mesenchymal-like, and small-cell- or neuroendocrine-like. Specimens can be classified as basal or luminal using GATA3 and KRT5 IHC, with >90% accuracy in comparison to mRNA genomic profiling [13]. The luminal subtype can be further subclassified as GU or URO by assessing p16 expression, which is enriched in GU and not in URO [12,13,15]. A three-antibody IHC subtyping classifier covering GATA3, KRT5, and p16 was recently developed and internally validated for both non–muscle-invasive bladder cancer (NMIBC) and MIBC [12.13]. The IHC-based molecular NMIBC subtypes were associated with differential risk of progression and recurrence.

Molecular subtyping data remain scarce for patients treated with radiation-based therapy (RT). The clinical response of various molecular subtypes has only been investigated in one study, which did not reveal a difference in survival among different subtypes [16]. Therefore, our study had two objectives: (1) to assess the feasibility of molecular subtyping for patients treated with RT for MIBC using the three-antibody based classifier and (2) to evaluate the association of IHC subtypes with clinical outcomes.

2. Patients and methods

After obtaining approval from the institutional research ethics board, we collected retrospective data on patient demographics, treatment outcomes, and pathology from the institutional database for a TMT cohort. Baseline information was obtained from medical records and included age, sex, Eastern Cooperative Oncology Group (ECOG) performance status, and follow-up time. Clinical and histopathological data included use of neoadjuvant chemotherapy, use of concurrent chemotherapy, presence of hydronephrosis, clinical tumor and nodal stage, presence of lymphovascular invasion, presence of carcinoma in-situ, complete response (CR), recurrence, and death. Complete versus incomplete transurethral resection of bladder tumor (TURBT) was defined using operative reports. CR was defined as the absence of carcinoma on tumor bed biopsy within 3 mo after RT and negative cross-sectional imaging. If biopsy was not performed, CR was defined as having both negative cystoscopy and cytology and no signs of locoregional tumor on cross-sectional imaging at 3 mo after treatment. Recurrence was defined as either locoregional or distant recurrence after no evidence of disease status at 3 mo. Recurrence status was assessed for patients at their last follow-up. Patients with tumor cores containing staining artifacts, slide edge effects, or insufficient tumor cell content were excluded.

2.1. Histopathology

For each patient, formalin-fixed, paraffin-embedded TURBT tissues were used to prepare tissue microarrays using 1.5-mm cores. Five cores per patient were used (2 from the center of the tumor, 2 from the edges, and 1 from normal urothelium). Only the tumor cores were included in the analysis. IHC analysis was based on the three-antibody algorithm described by Jackson et al. [12,13]. The IHC tumor cell score (TCS) for each marker was calculated using intensity staining for GATA3 and p16 and proximity scoring for KRT5. Intensity staining was scored on a scale from 0 to 3 according to visual assessment. Proximity was assessed according to proximity to the basal cell layer: no staining, score = 0; staining confined to the basal cell layer, score = 1; staining of basal and suprabasal layers, score = 2; and homogeneous staining, score = 3. The percentage of cells positive for each marker was calculated by deciles (0.1–0.9) using the HALO v2.1 image analysis platform (Indica Labs, Albuquerque, NM, USA). TCS was calculated as the product of the proximity/intensity score multiplied by the percentage of positive cells and divided by the maximum score of 2.7 $\left(\frac{\text{Staining score} \times \% \text{ positive cells}}{2.7}\right)$ to yield a TCS ranging between 0 and 1. The quality of the histopathological slides was assessed

by two blinded reviewers and a senior uropathologist. The potential risk of subtype misclassification due to tumor heterogeneity was minimized using two tumor cores from the same patient. In addition, a double staining method was used to identify focal heterogeneity between basal and luminal markers within the same section of tissue.

2.2. Statistical analysis

Descriptive data for the baseline characteristics of the cohort are presented as the frequency and percentage for categorical variables, and as the median or mean and interquartile range (IQR) or 95% confidence interval (CI) for continuous variables. To ensure homogeneous baseline characteristics between the molecular subtypes, the analysis-of-variance test was used to compare continuous variables. The χ^2 test and Fisher's exact test were used to determine if there were differences between patients with the different subtypes for categorical variables and ensure homogeneity of the groups. OS was calculated from the last day of RT to death from any cause. Recurrence-free survival (RFS) was calculated from the last day of RT until either distant or local recurrence. Patients were censored at the last follow-up date. Log-rank tests and Kaplan-Meier curves were used to estimate RFS and OS. Quantitative variables were tested for the log linearity hypothesis, and the proportional hazards assumptions were verified for all variables. A two-sided level of significance of $p < 0.05$ was adopted for all tests. A multivariable model was generated using the variables deemed to be most predictive of outcomes specifically in patients with MIBC treated with RT.

Statistical tests were performed using SPSS for Macintosh v.27. Graphics and heatmaps were plotted using R for macOS v.4.1.2. Heatmaps were generated using hierarchical clustering with the complete linkage method and Euclidean distance. The optimal number of clusters was determined using the *nbclust* function. The average silhouette width was computed to measure the consistency of the data clusters.

3. Results

The clinicopathological characteristics and demographics of the cohort are summarized in Table 1. In total, 104 patients who underwent RT for MIBC were reviewed and 93 were included in the study analysis. The median age was 75 yr (IQR 65–80) and females comprised 23% of the patients. The median follow-up was 55 mo (IQR 39–75; events excluded). TURBT was deemed complete in 73% of the patients. Most patients had T2 disease (84%). Twenty patients (22%) received neoadjuvant chemotherapy before RT and 79 (85%) received concurrent chemotherapy as a radiosensitizer. Of the 14 patients who did not receive a radiosensitizing chemotherapeutic agent, five had received neoadjuvant chemotherapy. Three of these patients were later deemed unsuitable for further chemotherapy (1 because of a hip fracture, 2 because of general physical status). The other two refused further systemic therapy. For the nine patients who never received a systemic chemotherapeutic agent, refusal or poor candidacy for chemotherapy was the reason. A χ^2 test confirmed that there were no significant differences in categorical variables such as the presence of carcinoma in situ, lymphovascular invasion, or hydronephrosis between the MIBC subtypes. Similarly, Fisher's exact test confirmed that there were no significant differences in sex, ECOG performance status, T stage, neoadjuvant chemotherapy, complete TURBT, or concurrent chemotherapy (Table 2).

Table 1 – Demographics and baseline characteristics of patients with subtyped tumors (*n* = 93)

Variable	Result[a]
Median age, yr (IQR)	75 (65–80)
Male, *n* (%)	72 (77)
Median follow-up, mo (IQR)	55 (39–75)
ECOG PS, *n* (%)	
0	43 (46)
1	28 (30)
2	17 (18)
3	4 (4.3)
Clinical tumor stage, *n* (%)	
cT2	78 (84)
cT3	10 (11)
cT4	3 (3.3)
Positive clinical nodal stage, *n* (%)	11 (12)
Lymphovascular invasion, *n* (%)[b]	27 (29)
Carcinoma in situ, *n* (%)[b]	34 (37)
Hydronephrosis, *n* (%)	21 (23)
Neoadjuvant chemotherapy, *n* (%)	20 (22)
Complete TURBT, *n* (%)	68 (73)
Concurrent chemotherapy, *n* (%)	79 (85)
Molecular subtype, *n* (%)	
Basal	22 (24)
Luminal	42 (45)
Genomically unstable	13 (14)
Urothelial-like	29 (31)
Negative/unclassified	29 (31)

ECOG PS = Eastern Cooperative Oncology Group performance status; IQR = interquartile range; TURBT = transurethral resection of bladder tumor.
[a] Numbers may not add up owing to missing information for a minority of patients.
[b] Yes versus no/not mentioned/cannot be assessed.

3.1. Staining assessment, subtype assignment, and tumor heterogeneity

Representative patient tumors stained for each subtype are presented in Figure 1. We excluded 11 patient cores with a low cell count, staining artifacts, or diffuse variant histology. GATA3 and KRT5 staining was performed on the same slide, while p16 staining was conducted on a different slide. Tumors exhibiting cytoplasmic KRT5 staining (pink) and negative GATA3 staining were classified as the basal subtype. Luminal tumors showed diffuse GATA3 staining and were negative for KRT5. Among the luminal tumors, those staining for p16 correspond to the luminal GU subtype and those negative for p16 to the luminal URO subtype. There was subtype agreement between cores for the majority of patients with two cores (94%).

3.2. Hierarchical clustering

The clustering dendrogram and heatmap are presented in Figure 2. The majority of patients (n = 93, 89%) had tumors that were successfully classified into one of six different clusters (average silhouette width 0.48). The heatmap shows the TCS for each marker, with scores between 0 (weak blue) and 1 (strong red). Clusters 1 and 2 represent KRT5-positive MIBC, corresponding to the basal molecular subtype (n = 22, 24%). Cluster 3 represents GATA3- and p16-positive MIBC, corresponding to the luminal GU subtype (n = 13, 14%). Clusters 4 and 6 were negative for both GATA3 and KRT5; therefore, these MIBCs were clustered into the triple/double negative group (n = 29, 31%). Cluster

Table 2 – Demographics and baseline characteristics stratified by molecular subtype

Variable	Basal	Luminal		Negative	*p* value
		GU	URO		
Mean age, yr (95% CI)	74 (68–78)	71 (65–78)	71 (67–76)	72 (68–74)	0.9
Male, *n* (%)	15 (68)	12 (92)	25 (86)	20 (69)	0.16
ECOG PS, *n* (%)					
0–1	15 (68)	9 (69)	21 (75)	26 (89)	0.2
2–3	7 (31)	4 (30)	7(25)	3 (10)	
Clinical tumor stage, *n* (%)					0.5
Organ-confined	17 (77)	11 (85)	24 (83)	27 (93)	
Non–organ-confined	5 (23)	2 (15)	5 (17)	2 (6.9)	
Lymphovascular invasion, *n* (%)[a]	6 (27)	3 (23)	8 (29)	10 (35)	0.9
Carcinoma in situ, *n* (%)[a]	8 (36)	5 (39)	10 (36)	11 (38)	>0.9
Hydronephrosis, *n* (%)	5 (22)	2 (15)	8 (29)	6 (21)	0.8
Neoadjuvant chemotherapy, *n* (%)	4 (18)	4 (31)	6 (21)	6 (21)	0.8
Complete TURBT, *n* (%)	13 (59)	10 (77)	20 (74)	25 (86)	0.17
Concurrent chemotherapy, *n* (%)	16 (73)	11 (85)	24 (86)	28 (97)	0.13

CI = confidence interval; ECOG PS = Eastern Cooperative Oncology Group performance status; GU = genomically unstable; TURBT = transurethral resection of bladder tumor; URO = urothelial-like.
[a] Yes versus no/not mentioned/cannot be assessed.

5 represents GATA3-positive and p16-negative MIBC, corresponding to the luminal URO subtype (*n* = 29, 31%; Table 1).

3.3. Association between subtype and clinical outcomes

The proportion of patients experiencing CR was 84% (*n* = 20) in the basal group, 85% (*n* = 24) in the URO group, 78% (*n* = 10) in the GU group, and 65% (*n* = 18) in the double/triple negative group (*p* = 0.5). Kaplan-Meier results for OS and RFS are presented in Figure 3. There were no significant differences in median OS (34 vs 36 vs 59 mo; *p* = 0.6) or median RFS (not reached vs 22 vs 66 mo; *p* = 0.6) among basal versus luminal versus negative subtypes. Similarly, comparison of basal versus luminal subtypes revealed no significant difference in either OS (*p* = 0.8) or RFS (*p* = 0.4).

On multivariable logistic regression, molecular subtype was not associated with CR (65 patients with CR) or RFS (36 events). For OS, we included age, cT stage, concurrent chemotherapy, presence of CIS, and molecular subtype in the multivariable analysis, as these were deemed the most predictive variables for patients treated with RT [16]. Only age (HR 1.03, 95% CI 1.02–1.06; *p* = 0.041) and cT stage (HR 2.9, 95% CI 1.2–6.7; *p* = 0.014) were significantly associated with OS (51 events; Table 3).

4. Discussion

This study externally validated the three-antibody IHC algorithm for MIBC subtyping, which was successful in the majority of the study patients treated with RT. However, the classifier was not predictive for survival outcomes.

Data on molecular subtypes and their response to radiation-based therapy are scarce. Much of the current literature classifies MIBC subtypes via genomic sequencing or transcriptomic profiling, a costly method that is not widely available. Subtyping via IHC is an emerging cost-effective alternative more readily available in pathology laboratories. The challenge lies in determining the optimal combination and number of markers to classify patients into the various subtypes. Guo et al. [11] previously identified KRT5 and GATA3 as the two markers for most effective classification of tumors as basal or luminal subtypes (89% accuracy). Data on MIBC subtyping via IHC and correlation to mRNA expression profiling were validated for the Lund taxonomy: high sensitivity of the IHC-based molecular subtyping was observed for URO and GU tumors (0.89 and 0.79) and specificity of 93% for the basal subtype [15]. A more recent study further expanded on this classification and tested the accuracy of a three-antibody classifier covering GATA3, KRT5, and p16. This combination was >90% accurate in classifying MIBC samples as luminal and basal subtypes, and 78% accurate (95% CI 67–86%) in classifying basal, URO, and GU subtypes [13]. To the best of our knowledge, ours is the first study to demonstrate dual staining for GATA3 and KRT5 in this population, an approach that facilitates luminal-basal subtyping on a single slide. Given the emerging role of IHC in molecular subtyping, we sought to investigate the utility and feasibility of the three-antibody molecular classifier in our TMT database. The IHC classifier was able to subtype 89.4% of patients with MIBC treated with RT. A fraction of patients in this cohort were classified as having a "negative" subtype, as their tumors did not stain for either GATA3 or KRT5, or stained with insufficient intensity to cluster with the other subgroups. Despite no statistically significant difference in survival, it was previously shown that tumors of this subtype are associated with worse prognosis with surgical management across studies [17]. These tumors tend to lose epithelial differentiation and underexpress claudin-related genes, which promotes an immunosuppressed environment [18]. Although they lack features suggestive of luminal-like tumors, they are also evidently distinct from the basal/squamous subtype. Furthermore, these tumors frequently exhibit variant morphology, classifying them as mesenchymal-like or neuroendocrine-like according to the Lund taxonomy, and they may therefore be identifiable with the use of additional IHC stains. Multiple reasons may explain the lack of significant differences in survival for the negative tumors in our study. For instance, the heatmap demonstrates that tumors from multiple patients in clusters 4 and 6 (double and triple

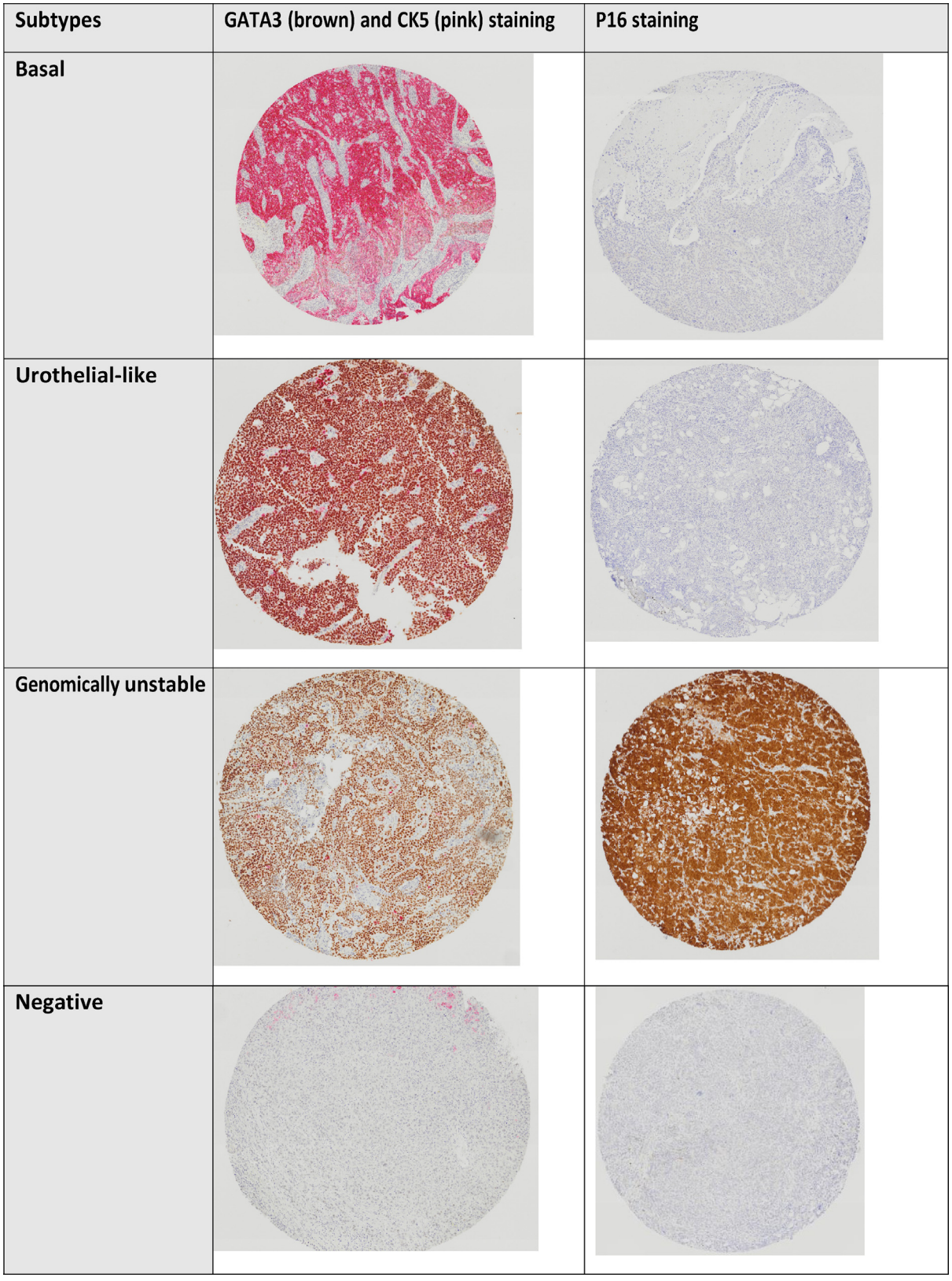

Fig. 1 – Examples of patient tumors of the basal, urothelial-like, genomically unstable, and negative subtypes.

negatives) stained positively, albeit weakly, for GATA3/KRT5. It could be argued that the more sensitive mRNA-based classifier might have clustered these tumors differently. Conversely, these tumors may have derived more benefit from RT and, consistent with Efstathiou et al [16], achieved similar survival to the other subtypes. Future

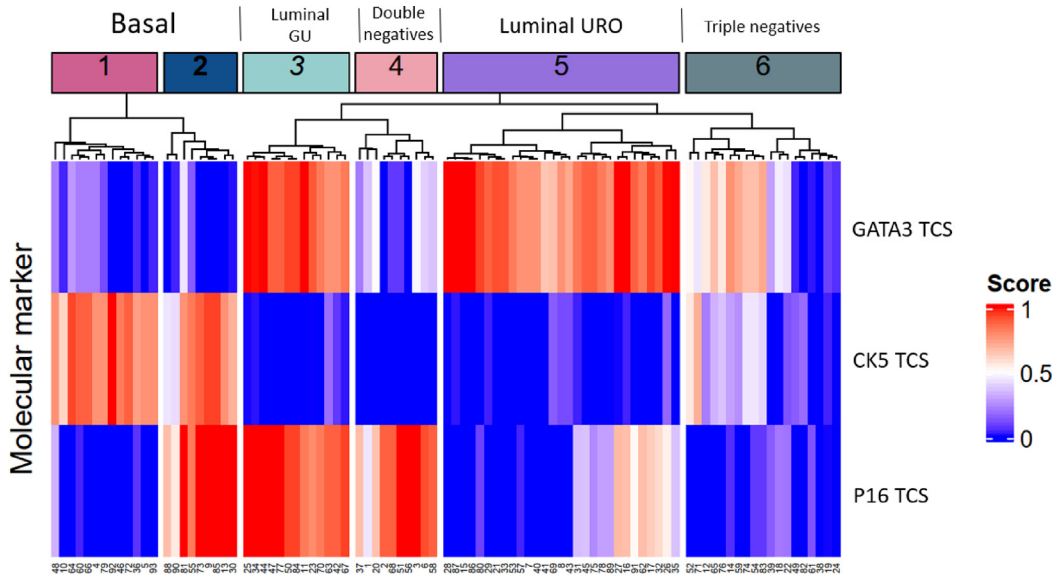

GU – genomically unstable; URO – urothelial like; TCS - tumor cell score

Fig. 2 – GATA3, CK5, and P16 heatmaps for each patient and clustering dendrogram. GU = genomically unstable; URO = urothelial like; TCS = tumor cell score.

1. Kaplan-Meier analysis for OS (left) and RFS (right) comparing basal, luminal and negative subgroups

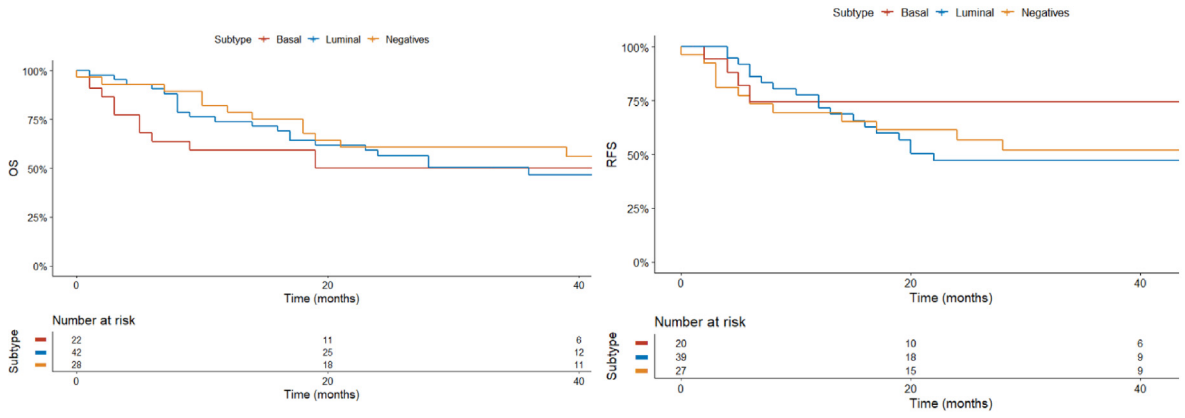

2. Kaplan-Meier analysis for OS (left) and RFS (right) comparing basal and luminal subgroups

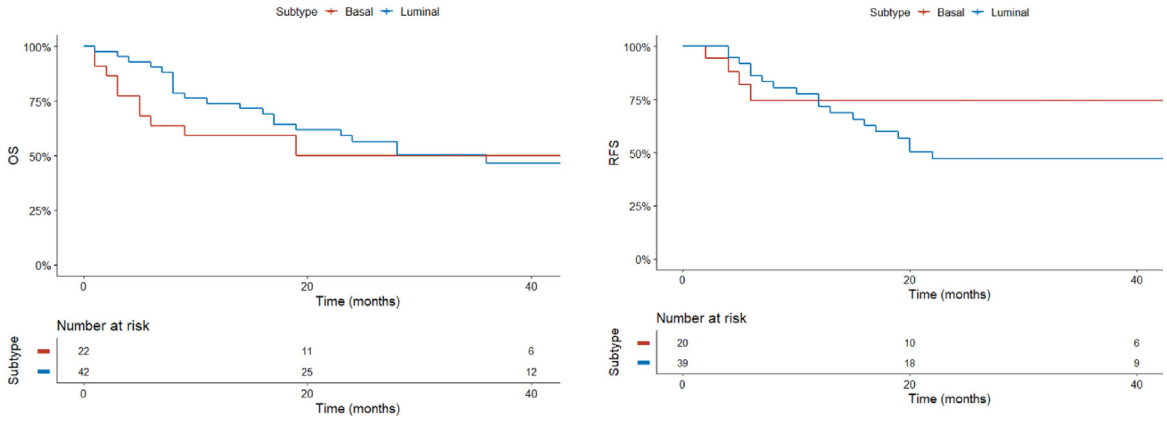

Fig. 3 – Comparison of (A) overall survival and (B) recurrence-free survival for the basal, luminal, and negative subgroups, and (C) overall survival OS and (D) recurrence-free survival for the basal and luminal subgroups according to Kaplan-Meier analysis.

Table 3 – Multivariable analysis for overall survival, recurrence-free survival, and complete response

Variable	HR (95% CI)	*p* value
Overall survival		
Age	1.03 (1.02–1.06)	0.041
cT stage	2.9 (1.2–6.7)	0.014
Concurrent chemotherapy	0.9 (0.4–2.1)	0.8
Carcinoma in situ	0.9 (0.6–1.4)	0.7
Molecular subtype (basal vs others)	0.9 (0.4–1.6)	0.6
Recurrence-free survival		
cT stage	2.0 (0.7–5.9)	0.2
Concurrent chemotherapy	4.3 (0.5–35)	0.17
Molecular subtype (basal vs others)	1.6 (0.62–4.1)	0.3
Complete response		
cT stage	1.0 (0.33–16)	0.8
Concurrent chemotherapy	0.97 (0.5–26)	0.2
Molecular subtype (basal vs others)	0.79 (0.06–1.5)	0.2

CI = confidence interval; HR = hazard ratio.

larger-scale studies including a treatment control group are necessary to further clarify this finding. As demonstrated here, an inexpensive and rapid IHC test for molecular subtyping should facilitate such studies.

The literature on breast cancer molecular subtypes and their response to RT is more established than that on bladder cancer. Several studies have shown that the basal subtype in breast cancer is associated with radioresistance and a higher rate of local recurrence (7.1% vs 0.8% for the luminal A and 1.5% for the luminal B subtype) [19,20]. Another study found that among patients with breast cancer metastasis treated with targeted therapy, median OS was significantly shorter for patients with the basal subtype versus luminal A and luminal B subtypes (8.4 vs 12.3 vs 18.8 mo; $p < 0.001$) [21]. We did not find significant differences in either OS or RFS after RT-based therapy among the MIBC molecular subtypes. These findings are consistent with the results of Efstathiou et al. [16], who observed no differences in OS ($p = 0.5$) or disease-specific survival ($p = 0.8$) when comparing basal, luminal, and claudin-low (equivalent to the negative subgroup in this study) subgroups. Larger prospective studies over longer follow-up are necessary to confirm the lack of difference in survival between different molecular MIBC subtypes treated with RT.

4.1. Limitations

The retrospective nature of our study and relatively small sample size constitute inherent limitations. Furthermore, although subtyping via IHC is a simple alternative to genomic-based approaches, it remains a semi-qualitative method given the observer bias in scoring the staining pattern for each marker. Tumors strongly staining for a particular marker are easily subtyped, whereas tumors staining for multiple markers and/or weakly staining for one marker represent a challenge with this method. We reduced this bias by having blinded reviewers assess each tumoral slide and assign a score for each marker.

Intratumoral heterogeneity may affect the ability of staining algorithms to reliably classify patient tumors into molecular subtypes. Warrick et al. [22] demonstrated that up to 39% of cystectomy samples with histological variants displayed staining heterogeneity when using the Lund IHC methodology. This finding was mainly noted for the basal squamous subtype. The authors detected no co-occurrence of URO and GU in the same patient. Their subtyping was performed on cystectomy specimens, which exhibit greater staining heterogeneity owing to the longer fixation times in comparison to TURBT specimens and can be particularly evident for luminal markers such as GATA3 [23]. In addition, molecular subtyping of NMIBC using the Lund taxonomy showed 86% sample agreement on subtype [9]. To minimize tumor heterogeneity in the current study, we used the TURBT specimen and double staining for GATA3 and CK5 for multiple cores from each tumor.

Future larger-scale studies could incorporate genomic sequencing along with IHC for whole tumor specimens to better characterize tumors and further validate the reliability of the three-antibody classifier.

5. Conclusions

IHC profiling of molecular MIBC subtypes in patients treated with RT was successful for most tumors using only three antibodies. This study is the first to successfully classify such tumors treated with RT based solely on IHC. There was no association between subtype and survival or CR. Future larger-scale prospective studies may help in validating the lack of association between these subtypes and prognosis.

Author contributions: Wassim Kassouf had full access to all the data in the study and takes responsibility for the integrity of the data and the accuracy of the data analysis.

Study concept and design: Hesswani, Jackson, Marcq, Mansure, Berman, Kassouf.
Acquisition of data: Hesswani, Jackson, Marcq, Hardy, Brimo.
Analysis and interpretation of data: Hesswani, Jackson, Marcq, Kool, Berman, Kassouf.
Drafting of the manuscript: Hesswani, Kassouf.
Critical revision of the manuscript for important intellectual content: Hesswani, Jackson, Marcq, Kool, Mansure, Berman, Kassouf.
Statistical analysis: Hesswani, Marcq, Kool.
Obtaining funding: None.
Administrative, technical, or material support: Hesswani, Hardy, Mansure, Brimo.
Supervision: Berman, Kassouf.
Other: None.

Financial disclosures: Wassim Kassouf certifies that all conflicts of interest, including specific financial interests and relationships and affiliations relevant to the subject matter or materials discussed in the manuscript (eg, employment/affiliation, grants or funding, consultancies, honoraria, stock ownership or options, expert testimony, royalties, or patents filed, received, or pending), are the following: None.

Funding/Support and role of the sponsor: None.

References

[1] Gakis G, Efstathiou J, Lerner SP, et al. ICUD-EAU international consultation on bladder cancer 2012: radical cystectomy and

bladder preservation for muscle-invasive urothelial carcinoma of the bladder. Eur Urol 2013;63:45–57.
[2] Kulkarni GS, Hermanns T, Wei Y, et al. Propensity score analysis of radical cystectomy versus bladder-sparing trimodal therapy in the setting of a multidisciplinary bladder cancer clinic. J Clin Oncol 2017;35:2299–305.
[3] Fahmy O, Khairul-Asri MG, Schubert T, et al. A systematic review and meta-analysis on the oncological long-term outcomes after trimodality therapy and radical cystectomy with or without neoadjuvant chemotherapy for muscle-invasive bladder cancer. Urol Oncol 2018;36:43–53.
[4] Seisen T, Sun M, Lipsitz SR, et al. Comparative effectiveness of trimodal therapy versus radical cystectomy for localized muscle-invasive urothelial carcinoma of the bladder. Eur Urol 2017;72:483–7.
[5] Choi W, Czerniak B, Ochoa A, et al. Intrinsic basal and luminal subtypes of muscle-invasive bladder cancer. Nat Rev Urol 2014;11:400–10.
[6] Bernardo C, Eriksson P, Marzouka NAD, Liedberg F, Sjödahl G, Höglund M. Molecular pathology of the luminal class of urothelial tumors. J Pathol 2019;249:308–18.
[7] Kamoun A, de Reyniès A, Allory Y, et al. A consensus molecular classification of muscle-invasive bladder cancer. Eur Urol 2020;77:420–33.
[8] Robertson AG, Kim J, Al-Ahmadie H, et al. Comprehensive molecular characterization of muscle-invasive bladder cancer. Cell 2017;171:540–556.e25.
[9] Sjödahl G, Jackson CL, Bartlett JM, Siemens DR, Berman DM. Molecular profiling in muscle-invasive bladder cancer: more than the sum of its parts. J Pathol 2019;247:563–73.
[10] Eriksson P, Rovira C, Liedberg F, Sjödahl G, Höglund M. A validation and extended description of the Lund taxonomy for urothelial carcinoma using the TCGA cohort. Sci Rep 2018;8:3737.
[11] Guo CC, Bondaruk J, Yao H, et al. Assessment of luminal and basal phenotypes in bladder cancer. Sci Rep 2020;10:9743.
[12] Jackson CL, Chen L, Hardy CS, et al. Diagnostic and prognostic implications of a three-antibody molecular subtyping algorithm for non-muscle invasive bladder cancer. J Pathol Clin Res 2022;8:143–54.
[13] Hardy C, Ghaedi H, Slotman A, et al. Immunohistochemical assays for bladder cancer molecular subtyping: optimizing parsimony and performance using Lund taxonomy. J Histochem Cytochem 2022;70:357–75.
[14] Sjödahl G. Molecular subtype profiling of urothelial carcinoma using a subtype-specific immunohistochemistry panel. Mehods Mol Biol 2018;1655:53–64.
[15] Sjödahl G, Eriksson P, Liedberg F, Höglund M. Molecular classification of urothelial carcinoma: global mRNA classification versus tumour-cell phenotype classification. J Pathol 2017;242:113–25.
[16] Efstathiou JA, Mouw KW, Gibb EA, et al. Impact of immune and stromal infiltration on outcomes following bladder-sparing trimodality therapy for muscle-invasive bladder cancer. Eur Urol 2019;76:59–68.
[17] Seiler R, Ashab HAD, Erho N, et al. Impact of molecular subtypes in muscle-invasive bladder cancer on predicting response and survival after neoadjuvant chemotherapy. Eur Urol 2017;72:544–54.
[18] Kardos J, Chai S, Mose LE, et al. Claudin-low bladder tumors are immune infiltrated and actively immune suppressed. JCI Insight 2016;1:e85902.
[19] Nguyen PL, Taghian AG, Katz MS, et al. Breast cancer subtype approximated by estrogen receptor, progesterone receptor, and HER-2 is associated with local and distant recurrence after breast-conserving therapy. J Clin Oncol 2008;26:2373–8.
[20] Huber KE, Carey LA, Wazer DE. Breast cancer molecular subtypes in patients with locally advanced disease: impact on prognosis, patterns of recurrence, and response to therapy. Semin Radiat Oncol 2009;19:204–10.
[21] Miller JA, Kotecha R, Ahluwalia MS, et al. Overall survival and the response to radiotherapy among molecular subtypes of breast cancer brain metastases treated with targeted therapies. Cancer 2017;123:2283–93.
[22] Warrick JI, Sjödahl G, Kaag M, et al. Intratumoral heterogeneity of bladder cancer by molecular subtypes and histologic variants. Eur Urol 2019;75:18–22.
[23] Pardo JC, Ruiz de Porras V, Plaja A, et al. Moving towards personalized medicine in muscle-invasive bladder cancer: where are we now and where are we going? Int J Mol Sci 2020;21:6271.